Fusion Engineering and Design 122 (2017) 365–374

Contents lists available at ScienceDirect

Fusion Engineering and Design

journal homepage: www.elsevier.com/locate/fusengdes

Diagnostics, data acquisition and control of the divertor test tokamak experiment

R. Albanese[a], R. Ambrosino[b], M. Ariola[b], G. De Tommasi[a], A. Pironti[a], M. Cavinato[c], A. Neto[c], F. Piccolo[c], F. Sartori[c], R. Ranz[c], L. Carraro[d], A. Canton[d], R. Cavazzana[d], A. Fassina[d], P. Franz[d], P. Innocente[d], A. Luchetta[d], G. Manduchi[d], L. Marrelli[d], E. Martines[d], S. Peruzzo[d], M.E. Puiatti[d], P. Scarin[d], G. Spizzo[d], M. Spolaore[d], M. Valisa[d,*], G. Gorini[e], M. Nocente[e], C. Sozzi[f], M.L. Apicella[g], L. Gabellieri[g], G. Maddaluno[g], G. Ramogida[g]

[a] CREATE, Università di Napoli "Federico II", Italy
[b] CREATE, Università di Napoli "Parthenope", Italy
[c] F4E, Barcelona, Spain
[d] Consorzio RFX, Padova, Italy
[e] Università di "Milano-Bicocca", Italy
[f] IFP CNR Milano, Italy
[g] ENEA Frascati, Italy

ARTICLE INFO

Article history:
Received 11 August 2016
Received in revised form 24 May 2017
Accepted 24 May 2017
Available online 11 August 2017

Keywords:
Power exhaust
Plasma control
Diagnostics
Data acquisition

ABSTRACT

The system of diagnostics, data acquisition and control foreseen on the Divertor Test Tokamak experiment (DTT) is presented. Conceived in an integrated way, the control system meets the specifications of a fusion experiment devoted to the study of the power exhaust problem in view of DEMO. Diagnostics and feedback control are particularly functional to the need of maintaining the plasma close to equilibrium in situations prone to instabilities where the plasma wall interaction is optimized. Strongly oriented to the exploration of control methods suitable for DEMO, DTT will specifically experiment on physics and engineering model based control systems. Control and data flow schemes are inspired by those of ITER.
© 2017 Elsevier B.V. All rights reserved.

1. Introduction

The specific mission of the Divertor Test Tokamak [1] will be to explore viable solutions to the power exhaust issues in a fusion reactor in view of DEMO. The ultimate goal will be to qualify and control in various divertor configurations DEMO relevant heat flux densities to the wall in a way that preserves both the integrity of the plasma facing components and the quality of the plasma performance. In this paper, we describe the initial approach to the system of diagnostics, data acquisition and control infrastructure foreseen on DTT. Sensors, actuators, models and communication infrastructures are conceived in an integrated way in order to assure that the many interlaced functions of a complex fusion device, such as plasma control, machine-protection and safety, are fulfilled simultaneously. Whereby some redundancy is foreseen for model validation and reliable feedback control purposes it is important to bear in mind that one of the ultimate goals of DTT will be to explore DEMO relevant ways to control complex situations, which is with a minimal amount of direct measurements of the plasma parameters. This is to be accomplished by relying more and more on physics and engineering models driven controls [2].

The compatibility of the diagnostics with the present machine design has been verified particularly with regard to the geometry and paying attention to several other important specifications such as electromagnetic and radiation compatibility as well as maintenance issues. However a detailed and exhaustive verification of all these aspects is beyond the scope of this work.

In Chapter 2, the diagnostics system is described, mainly in terms of their functionalities and their main specifications. A set of fundamental diagnostic has been selected for both the develop-

* Corresponding author.
E-mail address: Valisa@igi.cnr.it (M. Valisa).

http://dx.doi.org/10.1016/j.fusengdes.2017.05.118
0920-3796/© 2017 Elsevier B.V. All rights reserved.

ment of the scientific basis of the experiment, the protection of the machine and the stable operation of the discharge under robust real time control. Chapter 3 describes in more details some of the principal situations where feedback control will be necessary for assuring long pulses, with particular reference to the specific mission of DTT. Data acquisition and control system that have been conceived according to modern schemes and tools are illustrated in Chapter 4 before some final remarks.

2. The DTT diagnostics

The main DTT diagnostics so far conceived for DTT are listed in Table 1, grouped according to the parameters to be measured and in Table 2 Table 2, organized in terms of their use for feedback control purposes. A brief description of the most relevant diagnostic systems is given. The specifications of the diagnostics are conceived in order to assure an adequate documentation of both core and edge plasmas. At the edge the diagnostics set up has to be able to qualify in the various divertor scenarios the space distribution of radiation, impurities and heat fluxes, identify the degree of plasma detachment, evaluate the level of impurity compression and plasma enrichment. In the core, particle and energy confinement, impurities and radiation have to be documented in all of the divertor solutions. Diagnostics sensor and actuators must allow control of the instabilities that deviate the system from a given equilibrium, such as vertical and radiation instabilities.

2.1. Magnetic diagnostic

The magnetic diagnostics are relevant to all of the basic functions (machine protection, plasma control, physics studies and performance evaluation). Sub-systems may be conceived on the basis of the different measurement techniques: Magnetic flux sensors; Magnetic field probes; Current transducers. Several plasma parameters can be deduced by a combination of different magnetic sub-systems, which can have therefore different roles in the architecture of the magnetic diagnostic (primary, backup, supplemental).

Exhaustive literature about generic magnetic diagnostics can be found in [3] but in general the DTT design inspires to the specific design of ITER [4]. A preliminary estimate of the total number of magnetic sensors for DTT is expected to be of the order of one thousand (in between the number of sensors presently exploited at JET [5] and those foreseen for ITER [6], that is approximately 500 and 1500 respectively). The design and manufacturing of magnetic sensors for DTT could also benefit from recent developments for ITER [7,8], such as loops and windings made of Mineral Insulated Cables (MIC) and magnetic field probes based on Low-Temperature co-fired Ceramics technology LTCC with pickup coils more compact and less sensitive to detrimental radiation induced effects.

2.2. Plasma equilibrium and shape

Besides the standard magnetic measurements (probes and saddle coils) several diagnostics will be integrated in equilibrium reconstruction models to evaluate equilibrium and plasma shape including the interferometer–polarimeter and CCD cameras. Here we describe in particular the interferometer polarimeter.

Interferometer-polarimeter

Two interferometer-polarimeter systems are foreseen: a few channels mid infrared (MIR) 10 μm: a 5 μm CO2/CO *toroidal* system and a higher spatial resolution *poloidal* far infrared (FIR) one. The MIR vibration compensation scheme successful in both FTU and RFX-mod devices provides the reliable real time measurement of the chord averaged electron density [9]. The multi-chord FIR system measures the density and the plasma current profile (see Fig. 1). In the low/medium density cases, the FIR system will provide a good magnetic field measurement and the MIR one will provide vibration compensation for density measurement, while in the high density case the short wavelength alone can provide magnetic field measurement from Faraday rotation and density measurement from the Cotton-Mouton effect. Optimal laser source solution for polarimetric measurements resilient to density gradients is the 100/50 μm one. Optically pumped CH3OH 118 μm gas lasers are commercially available (e.g. at RFX-mod). Gas laser sources in the 50 μm range are yet unavailable but the so called THz domain of QCL lasers is progressing. A conservative solution would be to use a 10.6 μm CO2 laser for the vibration compensation (Table 2).

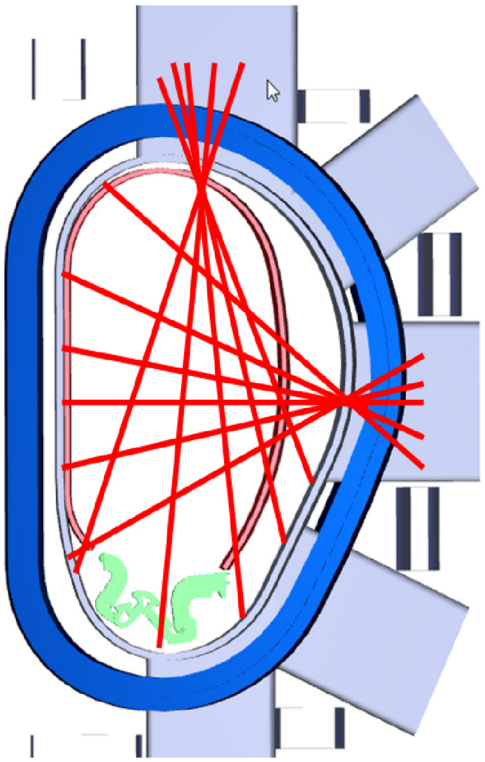

Fig. 1. interferometer-polarimeter viewing chords.

2.3. Core kinetic profiles and fast particles

Several diagnostics are foreseen to document the kinetic content of the plasma core and the presence of non-Mawellian components in the particles energy distribution, the latter being particularly important for their possible impact on plasma wall interactions. Besides a Thomson Scattering system an ECE radiometer, charge exchange spectroscopy and a crystal spectrometer have been considered, while fast particles will be monitored by

ECE radiometer

Suitable not only for electron temperature measurements, but also for MHD qualification, kinetic profile analysis and pedestal characterization, preliminary evaluations of the ECE radiation as detected by an antenna located at R = 3. 25 m, z = 0.15 m and radial line of sight have been performed. Both 1st harmonics, O mode (O1: 130 < f < 250 GHz) and 2nd harmonics, X mode (X2: 260 < f < 380) spectral regions are detectable with adequate radial resolution, of 1 cm for the X2 and 2 cm for O1, respectively. The X2 has appropriate resolution for spatial detection of the MHD activity. O1 measurements in the HFS might be used for the characterization of the kinetic quantities in the pedestal.

Charge exchange spectroscopy

Table 1
Main DTT diagnostics.

Parameter	Diagnostic	Characteristics	Resolution	Parameter	Diagnostic	Characteristics	Resolution
Magnetic diagnostics							
Magnetic Flux	Flux Saddle and diamagnetic Loop		0.1 ms	Magnetic Field	Pick up coils, Hall probes,polarimeter	MIC, LTCC Technology	0.1 ms
Halo/Hiro Currents	Rogowski coils, Resistive Shunts		0.1 ms	Plasma Current	Rogowski coils		0.1 ms
Plasma equilibrium and shape							
q Profile	FIR Polarimeter	Multichord	0.01 ms	Plasma Position and Shape	Flux and saddle loops, magnetic probes		0.1 ms
	MSE		10 cm, 10 ms				
	MagneticProbes		0.1 ms		CCD Imaging	Interf. filters	10–20 ms
Core kinetic profiles and fast particles							
Te Core	Thomson Scattering	Interf. filters spectrometer	10 cm, 10 ms	Ne Core	Thomson scattering	Internal optics required	10 cm, 10 ms
	ECE: O1 covers the full radial profile, X2 covers the LFS up to the centre	O mode (O1: 130 < f < 250 GHZ) and 2nd harmonics, X mode (X2: 260 < f < 380) detectable	1–2 cm FW @ 1/e, 0.1 ms	Real Time Ne Core	MIR Interferometer/FIR polarimeter	Few chords MIR, high resolution FIRInternal optics, QCL lasers	0.1 ms, 1 cm–10 cm
Ti	Crystal spectrometer	Ar for Te< 5 keV, Kr otherwise	20 cm, 10 ms	Fast Ions	NPA		5 ms
	CXRS	Diagnostic Beam-Impurities and Dα	50 ms		CXRS		10 ms
Ion Flow Plasma Core	Crystal spectrometer	Geometry	20 cm	Escaping Fast Ion	Scintillator probes		1 ms
	CXRS		10 ms		Faraday cups		1 ms
Runaway electrons	HXR/γ-Rays			Runaway electrons	Visible Spectrum	Co- and counter current views	10 ms
Neutrons and γ							
Neutron Yield	Fission chambers		10 ms	Neutron emission profile	Camera/Scintillators & Diamond Detector	From low to high neutron yield (1.3×10^{17} n/s)	10 ms
	TOF & LaBr3 γ detector camera	Neutron and γ cameras can be integrated	1 s/0.1 ms				
Core Radiation							
Radiation	ECE		0.1 ms	SXR diodes array			3 cm, kHz
SXR tomography			0.1 ms	Bolometer array	Metal foil/AXUV		2 cm, ms
Core impurities							
Zeff	Interference filters 5235.5 A and	Tangential chords and viewing dumps	0.1 ms	&	Low resolution spectrom.	Tangential chords and viewing dumps	10 ms
Line emission	VUV survey spectrom.	100–1200 A	10 ms	&	Crystal Spectrom.	A	10 ms
	Laser blow off	Target layers	Multipulse	&	XUV spectrom.	10–340 A	10 ms
Divertor diagnostics							
Divertor Te	Thomson Scattering	Standard	<1 cm, 10 ms	Neutrals	Fast baratron		ms
Compression/Enrichment	Spectros.	Ar, He Lines ratio	1 cm, <10 ms		RGA		100 ms
	Langmuir probes		1 cm, 1 ms		Filtered CCD cameras		10 ms, 2 mm
	Penning gauge spectrosc.	Magnetic Field screened	10 ms		NPA(TOF)	Energy lower limit	5 ms
Divertordetatchment	Visible Survey spectrom	Imaging mode	2 mm in imaging mode	&	VUV/VIS/NIR spectrum	Ionization, Balmer & Paschen series	10 ms, >1 cm
	Heterodyne Doppler		3 mm	&	Filtered CCD	3Dimaging software development	2 mm, 10 ms
	High resolution spectrum		10 ms	Divertor Ti	Retarding field analyzer		1 ms
Plasma wall interactions and disruptions							
Wall temperature	IR camera	Impact of redeposition layers	ms	Wall Hot Spots	CCD monitor	Pattern recognition	1 mm
	instrumented tiles	Thermocouples, Langmuir probes	ms	Redeposition layers	Microbalance	Environment compatibility	100 ms
Vessel deformation	Strain sensors/optical sensors				LIBS		

Table 2
Main objectives of feedback control.

	Diagnostics	Actuators	Control scheme
Plasma Current	Rogowski Coils	Magnetic Flux	PID
Axisymmetric equilibrium	Pick up coils/loops	PF coils	PID; Physics Model based
Electron Density	Interferometer/polarimeter	Gas valves/Criopumps	PID
MHD/NTM,RWM	Pick-up coil, ECE ($\Delta\rho \leq 0.1$), SXR	ECE/Saddle coils, ECRH for NTM	PID; Physics Model
MHD/ELM control	Dα, Stored energy	Saddle coils, plasma shape, Vertical kicks, Pellets/RMP's	PID; Physics Model based
Plasma Detachment	IR Cameras/thermocouples/CCD cameras/spectroscopy/Thomson Scattering	Fast gas valves for D2 and impurities (placed near the strike points); Far-away valve acting on the core density	PID; Physics model
Radiation/Enrichment factors	Bolometer arrays, SXR arrays and VUV spectrometers for the core radiation; Bolometer cameras, spectrometers in the divertor region;	In-vessel coils; Plasma Shaping and position; ECRH for heating	PID
Divertor Heat Flux	Infrared cameras Langmuir probes and thermocouples embedded in the divertor plates Thomson scattering High speed cameras equipped with suitable interference filters Magnetic measurements		

The most common diagnostic to measure the ion temperature and the collective flow is Charge eXchange Recombination Spectroscopy. In DTT, in absence of a suitable heating beam a diagnostic beam is considered. Simulations show that a beam of more than 80 keV and of about 6 A of equivalent current are required to obtain sufficient active signal in the core. The presence of tungsten in the plasma facing components adds the extra complexity of a rich background spectrum.

Crystal spectrometer

An alternative system being considered to measure the ion temperature is the X-ray crystal spectrometer. The imaging detector can be well screened from harsh radiation as it looks at the plasma indirectly through a crystal grating and this feature makes it suitable for DTT. Recent progresses will be exploited: Large detectors (100×300 mm) have been developed for KSTAR, NSTX and EAST and will be used on ITER. The issue of wavelength calibration has been solved on C-mod in discharges with non-rotating plasma. The spatial resolution is determined by detectors (for C-mod pixel size 0.172×0.172 mm) and by the distance between plasma and crystal (for EAST <1 m).

Fast ions

Fast ion detection is important to establish the contribution of this components of the escaping particles to the overall power exhaust. For this purpose DTT will rely on γ-ray detection and on edge scintillator probes, with possible contribution for the Dopple shifted Balmer Alpha emission by neutralized fast particles.

Runaway electrons

Standard HXR/γ detectors are complemented by an imaging visible spectrometer detecting the spectrum emitted in the forward direction by relativistic electrons, adding information on the spatial origin of the fast particles [10].

2.4. Neutron, gamma and hard X-ray diagnostics

Given the high neutron yield of 1.3×10^{17} n/s expected in DTT a set of neutron counters [10,11], a neutron/γ-ray camera and high resolution neutron and gamma-ray spectrometers are deemed suitable to measure the neutron yield, the profile of neutron emission and the supra-thermal components (accelerated fuel or ^{3}He ion population) respectively. A time of flight instrument along a dedicated line of sight and with the improved design deployed at EAST [12] would provide the adequate sensitivity (10^{-4} of the main thermal neutron emission) to study energetic tails [13,14]. High efficiency liquid scintillator and less sensitive but robust single crystal diamond detectors [15] for neutrons and high purity germanium detector or $LaBr_3$ scintillators for γ-rays [16] would cover the whole dynamic range of neutron and γ-rays emission expected in DTT operations. Measurements of γ-ray emission generated from reactions between the energetic ions and impurities [17,18] will be carried out. The γ-ray and neutron cameras can be integrated like in JET. γ-ray detectors can be used also to measure the profile and spectrum of hard x-ray emission from runaway electrons.

2.5. Radiation and impurities

A large set of diagnostics will be devoted for the characterization of the impurty content of both the main plasma and divertor.

Bolometry, Soft X-Rays detectors, short wavelength spectrometers plus effective charge monitors will be able to track the impurities content and their spatial distribution in the various experimental conditions.

Bolometry

Bolometry is essential for real-time control and optimization of the divertor power exhaust. On DTT a geometrical solution compatible with centimeter space resolution tomography has been studied based on 3 main heads, each hosting three fans covering the plasma core and 3 additional heads directed towards the divertor, as shown in Fig. 2.

The choice of detectors is oriented towards the radiation hard metal foils developed for ITER [19]. Faster and compact AXUV Silicon photodiodes tested on ASDEX Upgrade [20] and on C-mod [21] could be introduced for time resolved information, although their performance degrades strongly over time.

Soft X-Ray radiation

Soft X-Ray tomography is a powerful tool to diagnose both impurity accumulation and MHD activity in the hot plasma core, such as ELMs, sawtooth activity, or Fast Particles induced instabilities, e.g. Toroidal Alfven Eigenmodes.

For DTT we envisage using the state of the art system designed for shaped plasmas on ASDEX Upgrade (8 pinhole cameras installed with about 200 lines of sight. Silicon diodes screened by a curved Be filter 75 μm thick). The required bandwidth is 1 MHz, in order to detect also high frequency MHD.

Zeff

To improve the reliability of effective charge measurements in the core, observations of the continuum emission along the toroidal direction around 523. 5 nm, are foreseen. This region of the spectrum is less affected by line contamination and light reflection

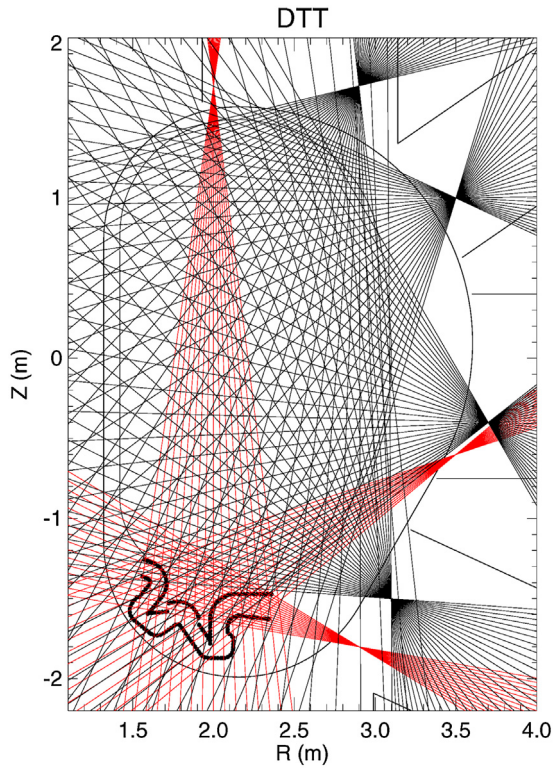

Fig. 2. Distribution of the bolometer arrays.

issues. Spectrally resolved surveys between 350 and 900 nm will be carried out to reveal the $1/\lambda^2$ dependence of continuum, of help against possible contaminations of the narrow band filter signal from several elements.

2.6. Divertor diagnostics

In line with the experiment mission, a particular attention is to be devoted to the diagnostics of edge and divertor region, focussing on impurity level, thermal characterization, plasma detachment, degree of enrichment of impurities, level of helium compression and power exhaust.

Charge exchange neutrals

Neutral particles play an important role at the edge of the plasma and in the divertor region hence in DTT two dedicated diagnostics are foreseen. Low energy escaping neutral particles will be detected by a time of flight (TOF) neutral particle analyser (NPA) with a path of around 4 m. The energy distribution information will be complemented by the analysis of the shape of the D alpha emission line as detected by a high resolution spectrometer. Coupling energy and density information yields the neutral pressure in the observed region.

Divertor Thomson scattering

In addition to the core Thomson Scattering system, a standard Thomson Scattering layout is specifically foreseen for the divertor, with fiber optics defining the scattered volume and interferential filter polychromators to analyse the signal. The main purpose is to detect plasma detachment states. A preliminary design maximizing solid angles, laser alignment reliability, minimizing stray light, optimizating spectral channel ranges, detectors and amplifiers seems to fit the requirements for the 1–10 eV Te range measurement, with densities around 1×10^{19} m^{-3}. Assuming efficiency values typical of the Thomson Scattering system of RFX-Mod, sufficient signal is expected. In Fig. 3 red dots show the proposed scattering volumes with sub centimeter resolution. Laser relays and collection optics

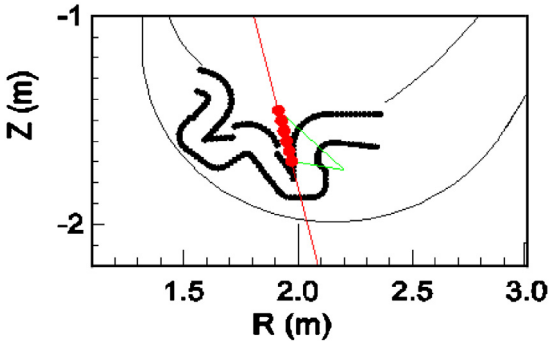

Fig. 3. Divertor Thomson Scattering Layout.

share the same mechanical support improving alignment reliability. Improvements of the layout, with multiple laser passages and laser dump outside the vessel are being considered, which would imply changes in the ports designs.

Divertor spectroscopy

Emission spectroscopy will be used on DTT as a multi-purpose tool in the divertor plasma, particularly useful to characterize detachment states (deuterium Balmer or Paschen series), plasma position and in general the kinetics of impurities and main gas (from Doppler broadening and shift). Two dimensional patterns of temperatures, ionization front and flows can be obtained by means of two-dimensional fast polarization interferometers [22]. As for other imaging systems, relays optics and detectors are to be positioned where they can be screened to neutrons.

Divertor and SOL probes

Insertable probes determine local kinetic parameters and turbulence microstructures. Both inner and outer divertor components will be equipped with Langmuir probes to detect particle fluxes, electron temperature and electron density and plasma flow. Retarding field analyzers will be used instead to characterize the ion temperature. Additionally a set of embedded treble coils to measure the electromagnetic radiation and its mode spectrum will allow the study of the discrete events that characterize the edge plasma, particularly during ELM events.

Plasma wall interaction monitoring system

The wall and the divertor will be monitored by a set of visible cameras and infrared cameras. Visible cameras are meant to serve as general monitor system during the discharge in particular with recognition capability of hot spots or abnormal events, but will be used also as detectors for real time control of the detachment phase and of the plasma position as a DEMO relevant alternative to magnetic probes or thermocouples. IR cameras will be installed to monitor surface temperature of PFC. Engineering models will be used to validate IR data, which are prone to yield overestimation of the bulk temperature in presence of loose redeposited layers on surfaces.

In situ PFC analysis

Laser Induced Background Spectroscopy (LIBS) with remote analysis capability and micro-destructive characteristics represents an ideal candidate to monitor the surface layer composition and the fuel gas content of the DTT plasma facing components. The feasibility of in-situ LIBS diagnostic of surface layer composition was demonstrated on FTU [23].

3. Real time control

3.1. Control and data acquisition system

DTT shares data acquisition and control requirements with other long lasting fusion experiments such as ITER and JT60SA. Long last-

ing plasma discharges require an approach in data acquisition that is radically different from that taken so far in most current machines (with a plasma duration up to 1 min), an approach where sensor and elaborated data are transferred to the to the experiment database during the discharge itself in order to allow the experimental team to have all the information necessary to take any necessary action in a timely manner.

The main technical implications of this new need are three: controllers need to be able to process real time data (from local or distributed sources) while at the same time be able to stream all the data out with a reasonable latency (<1s); data servers need to be able to collect the streaming data and update the database while users are concurrently accessing the existing pulse information; data visualization software need to be able to handle larger volume of data at the same time as new live visualization modes.

In addition to streamed data acquisition, the system must be able to use a subset of acquired signals for active control of the experiment. Real-time control systems for plasma discharge will impose different requirements that are less stringent on data throughput, but more demanding on data communication deadlines. As a consequence, a different communication bus will be defined for data used in real-time control, using an approach similar to the Synchronous Data Network (SDN) in ITER [24].

Plasma current, density, equilibrium, Beta, MHD control (Neoclassical Tearing Modes (NTM), Resistive Wall Modes (RWM), ELMs frequency and amplitude) and power exhaust control are some of the areas where feedback is to be applied. As an example of the studies performed for DTT, in the following section a conceptual design for the DTT plasma shape control system is presented.

The design is developed on the basis of *engineering-oriented* models which enable a model-based design of the control systems. Simpler than *physics-oriented* simulation codes, such as transport codes [2,25,26], such linear models permit also to automate both the validation and deployment of the plasma axisymmetric magnetic control [27–30] but are also used to support the design and commissioning of the plasma magnetic diagnostic [30], as well as to run inter-shot simulations aimed at optimising the controller parameters.

3.2. Model-based magnetic axisymmetric control

A state-space linear model [30–32] describing the behaviour of the plasma column and of the surrounding active and passive conductive structures is used to design the plasma magnetic axisymmetric control system for DTT and to estimate the power required to stabilize and control the plasma. The models are automatically generated around a given equilibrium by the CREATE 2D nonlinear equilibrium codes [33]. These type of models have been extensively validated against different fusion devices such as RFX [34], JET [35] and the EAST devices [36] and currently used also to perform preliminary studies and code benchmarking for both ITER [37] and DEMO [38]. It is worth noticing that the CREATE-NL+ equilibrium code [33] can be integrated with a transport solver [39].

In the following the best achievable performance in rejecting Vertical Displacement Events (VDEs), ELMs and H-L transitions is presented.

A preliminary architecture for the DTT magnetic control system is also proposed.

3.2.1. Architecture of the plasma axisymmetric magnetic control system

A block diagram of the overall magnetic control system architecture is reported in Fig. 4:

- *PF Current Decoupling Controller* guarantees that the currents in the PF circuits track the *scenario* references *currents* (feedforward action) requested by the outer control loops. The closed-loop bandwidth for the PF Current Decoupling Controller is mainly limited by the voltage limits of the power supplies and by the presence of the passive structures.
- *Plasma Vertical Stabilization Controller* stabilizes the vertically elongated and unstable plasma column by exploiting the in-vessel coils; The Vertical Stabilization Controller has in input the vertical velocity of the plasma centroid and the current flowing in the *C*5−*C*6 in-vessel coils pair, and generates as output the voltage references for these two copper coils (details on the DTT coils topology in [40]). If needed, in order to avoid current saturation in the in-vessel coils the superconductive PF coils can also used as actuators for vertical stabilization [41]
- *Plasma Current Controller* tracks the reference plasma current by driving a set of PF current deviations (with respect to the nominal values), which are proportional to a set of currents providing (in the absence of eddy currents) a *transformer field* inside the vacuum vessel, so as to reduce the coupling with the Plasma Shape Controller. In this architecture, the Plasma Current Controller is based on a simple proportional-integral-derivative (PID) controller.
- *Plasma Shape Controller* tracks a set of plasma shape descriptors and generates PF current deviation references to the PF Current Decoupling Controller. The plasma shape descriptors are usually computed by a plasma boundary reconstruction code, it computes a set of PF current. In the proposed architecture, an eXtreme Shape Control *XSC-like* approach is considered [42]. This approach has been proven effective to control high elongated plasma shapes both directly controlling the plasma-wall gaps [43] or by performing isoflux control [44]. By using an XSC approach it is possible to easily include current limit avoidance algorithms [40]. Furthermore, with the XSC it is possible to control simultaneously the plasma boundary and the flux expansion, and hence the heat load on the divertor, as it has been proposed for the EAST tokamak in [45].

Table 3
Maximum rejectable VDE when the IC5−IC6 coils pair is used to stabilize the plasma. The coil pair is assumed to be fed in anti-series with V_max=200 V and I_max=25 kA.

Equilibrium	equivalent VDE [*cm*]	t_{stop} [*ms*]
SN @42 s (high β_p)	∼2	∼5.1
QSF @ EOF	∼3	∼7.3
SF @ 42 s	∼7	∼15.6

3.2.2. Best achievable performance of the vertical stabilization system

Given the maximum values for the voltage and absolute current of the four quadrants power supplies for the *C*5–*C*6 in-vessel coils (200 V 25 kA, 100 kA/turn) [43], the model presented in Section 3.1 has been exploited to estimate the best achievable performance for the plasma vertical stabilization controller. First of all, the maximum rejectable VDE has been evaluated for a set of four different plasma equilibria. The results are summarised in Table 3, where, for each of the considered equilibria, the maximum rejectable VDE is reported together with the time t_{stop} needed to invert the plasma velocity.[1] It can be noticed that the maximum VDE is about 10 cm, while t_{stop} is always less than 10 ms. The performance of the vertical stabilization system β_p has been further assessed by considering the response to a 1.2 MJ ELM at high

[1] From the vertical stabilization point of view, a VDE is equivalent to a sudden and almost instantaneous change in plasma vertical position and velocity. It turns out that a VDE can be conveniently modeled as instantaneous change of the state in the linear model.

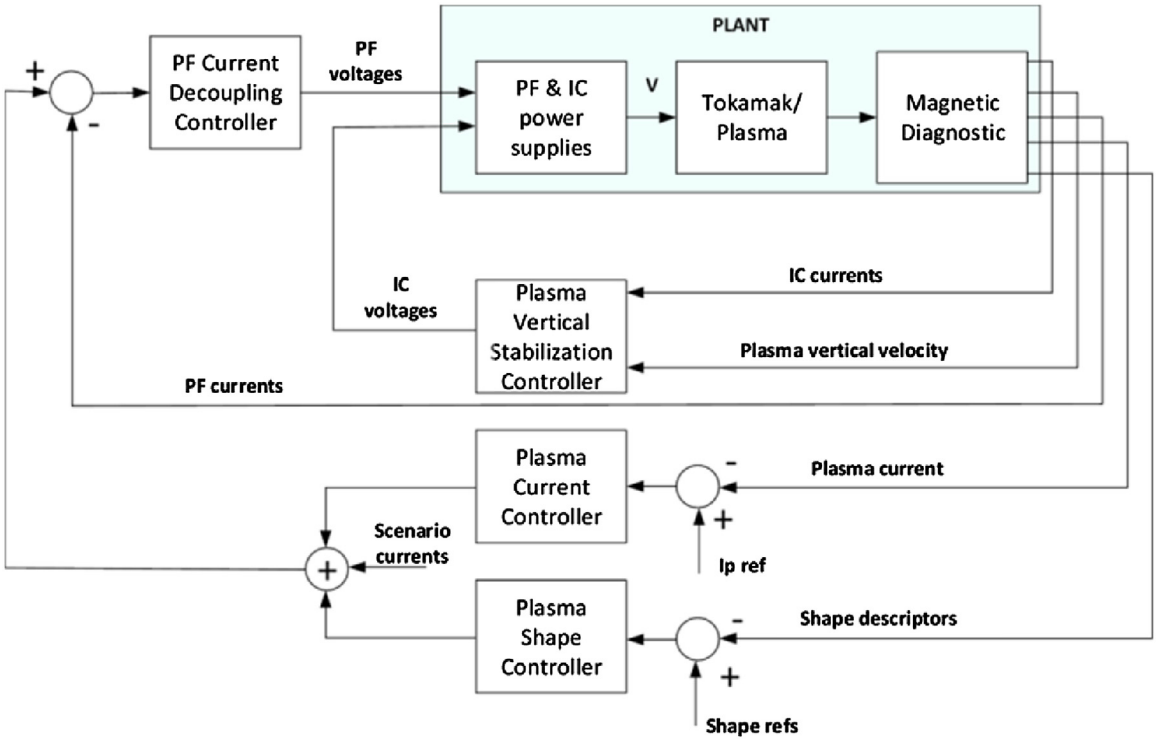

Fig. 4. Main blocks of the DTT magnetic control system architecture. The currents scenario represent the nominal PF current references designed offline and that are to be tracked by the PF Decoupling Controller, in order to obtain the desired plasma scenarios.

Table 4
Equivalent VDE and t_{stop} for a 1.2 MJ ELM. A vertical stabilization control system that uses the IC5–IC6 pair is considered. The coil pair is assumed to be fed in anti-series with V_{max} = 200V and I_{max} = 25kA. QSF is quasi Snow Flake, AF for Snow Flake and SN for Single Null geometry of the divertor X-point.

Equilibrium	equivalent VDE [cm]	maximum inboard displacement [cm]
SN @42 s (high β_p)	~1	~1
QSF @ EOF	~1	~1
SF @ 42 s	~2	~1

Such an ELM has been modeled as a poloidal beta drop

$$\Delta\beta_p = -\frac{8\Delta W_{DIA}}{3\mu_0 I_p^2} \cong -0.033,$$

and an increase of the internal inductance l_i given by $\Delta l_i = -\Delta\beta_p = 0.033$. This simplified model is used according to the specifications proposed for transients in ITER, which are based on JET experimental evidence. By exploiting again the linear model, an equivalent VDE has been computed for the considered ELM, together with the corresponding t_{stop}. The results are reported in Table 4, where it is shown that in this case the most challenging equilibria is the one corresponding to the snow-flake configuration. Eventually, similarly to what has been done for the 1.2 MJ ELM, the behaviour of the vertical stabilization system has been checked also against an H-L transition, which has been identified as a poloidal beta drop $\Delta\beta_p = -0.37$, and a drop of l_i of $\Delta l_i = -0.02$. The results are reported in Table 5, where the maximum inboard displacement is also given. In this case the vertical stabilization system shows good performance regardless of the considered equilibria. Moreover, it should be noticed that the inboard displacement would be further mitigated by the plasma shape controller.

Table 5
Equivalent VDE and t_{stop} for an H-L transition. A vertical stabilization control system that uses the IC5–IC6 pair is considered. The coil pair is assumed to be fed as in Table 4.

Equilibrium	growth rate γ [s^{-1}]	maximum VDE [cm]	t_{stop} [ms]
SN @32 s (low β_p)	~20.7	~10	~7.6
SN @42 s (high β_p)	~19.8	~12	~9.1
QSF @ EOF	~34.1	~11	~8.2
SF @ 42 s	~80.2	~9	~9.8

3.3. Power exhaust control

In the context of the exhaust control on DTT, the scenario of partially or completely detached plasma is of particular interest [46–53]. Core radiation will be monitored by a series of bolometer arrays, SXR arrays and VUV spectrometers, while in the divertor region three additional bolometer cameras are considered to enhance the local resolution capability to the cm level. The radiation diagnostics of the divertor are complemented by VUV to NIR spectrometers. Balmer and Paschen D series are indeed suitable to monitor the recombination process that occurs in the detachment phase, as demonstrated on C-Mod [54] and NSTX [55,56] while visible spectrometers measure the impurity influxes, which also decrease in the detachment phase. High speed cameras equipped with suitable interference filters can be used for real time optical plasma boundary reconstruction as shown on TCV [57]. Recently developed codes such as OFIT, allow for a fast, non-iterative analysis of the spectrally resolved images with low latency, to identify radiative shell edges in the image-emissivity [58]. In particular plasma boundary reconstructions of diverted plasma discharges have been obtained, showing agreement of about 1 cm with magnetic equilibrium reconstruction. Infrared cameras detect the heat flux profiles at inner and outer strike points. The set of diagnostics is complemented by Langmuir probes and thermocouples embedded in the divertor plates, which monitor particle and energy fluxes, a spa-

tially resolved (several millimeters) electron temperature profile measurements (Thomson Scattering) in the range 1–10 eV and by pressure gauges in the regions where pumps are located. The temperature measurements together with the magnetic measurements will be used by a feedback control algorithm acting on the currents in the in-vessel coils for the realization of the plasma advanced magnetic configurations (e.g. wobbling, strike point sweeping, etc.) and, more in general, for the control of the plasma strike point position and flux expansion. Regarding the possibility of having a detached regime in DTT, the main actuators are the fast gas valves for D2 and impurities placed near the strike points acting together with a far-away valve, which keeps the core density stationary. A fast heating system such as ECRH should compensate for overshoots of the radiative power.

The feedback loop for detachment control keeps the ionization front at a specified distance from the plates by regulating gas injection, based on the electron temperature profile measurements and/or other information from bolometry, cameras and spectroscopy, while the core density is maintained constant by a different loop. Bolometry is used to detect the possible formation of localized radiation condensation (MARFEs [59]). A similar technique has been demonstrated on DIII-D [60].

In addition, impurity accumulation in the core can be contained by ICRH and ECRH due to a variety of mechanisms – fast ion effects enhancing neoclassical screening, electron to ion heat flow ratio maximizing the turbulent transport [61].

Feedback systems will be firstly based on standard PID control. These systems have proven to be successful for example in DIII-D to control the detachment position.

Moreover, inclusion of the real-time plasma shape measurement by means of fast cameras (described above) in a feedback control loop for the plasma position, has demonstrated effective for the stabilization of the plasma vertical position. A real time analysis method for the plasma periphery has been demonstrated at 1 kHz with two cameras [46]. Ideally, a collisional-radiative model could calculate the emission for the different ionization stages and spectral transitions based on previous impurity density and local temperatures and the knowledge of the plasma composition and flag the proximity to operational limits or actuator constraints. To our knowledge however the first principle physics codes cannot yet predict the transition from attached to detached, and this represent an area of possible development.

3.4. MHD control

A provisional set up for Neoclassical Tearing Modes (NTM) and SawTooth (ST) control by means of the 170 GHz ECRH launching has been conceived by means of the codes GRAY (ECRH&ECCD) and SPECE (ECE) [62]. The system is based on 4 poloidally steerable 1 MW beams located in the upper port to minimize trapped electrons effects preserving the access to the HFS with Real Time capabilities. A toroidal steering between 10 and 15° appears to be feasible. Several hardware specifications have been defined: cooling requirements, antenna concept, diamond window, focussing optics, plug-in supporting structure. Optimized current drive efficiency at accessible radial ranges is obtained from the Upper port and at the q = 1, 3/2 and 2 surfaces has been estimated to be Icd = 9, 3.7 and 2.2 kA/MW respectively. The power and current drive radial localization Δr along the accessible radial range is $\Delta\rho \leq 0.1$, which is promising for the NTM stabilization.

As to the Resistive Wall Modes, specific modelling of active mitigation for safety purposes has not been carried out yet for DTT as it was for JT60-SA [63], which will be important to define the need and the specifications of the internal correction coils.

3.5. ELM control

Vertical kicks, pellets and Resonant Magnetic Perturbations, have all been successful in some way to pace the ELM in a controlled manner in various experiments. In a different approach the pedestal region is maintained in a state of quasi relaxed situation where no ELMs are generated. The I-mode in C-mod [62], the Quiescent H Mode [65] and Super H-mode [66] in DIII-D are such examples, all characterized by the presence of a continuous mode or broadband MHD spectrum. ELM-free plasma's in DIII-D are reached with sufficiently high EXB shear, which can be manipulated by means of the NBI torque and plasma shaping. The torque exerted by non-axisymmetric non-resonant magnetic perturbations has also been successful in reaching the QH mode with zero net NBI torque [64]. Injection of lithium, which modifies the edge density profile, has also lead to ELM free regimes in DIII-D [67]. Lower Hybrid Current Drive has been used on EAST to control ELMs [68]. Modelling of DTT scenarios is required to establish which technique is the most appropriate to stabilize ELMs, depending also on the systems available for the purpose. The use of internal coils for RMP production is in fact still under discussion.

4. DTT instrumentation & control system DICS

A brief survey of the main preliminary choices made to integrate tools and control system of DTT is given below.

Main functions

A modern fusion device is a large and complex civil and mechanical construction surrounded by a number of industrial plants which are meant to supply the necessary fuelling, power, and cooling to the tokamak load assembly standing at the centre of it all. Essential both for the operation of each component and for the coordination of the ensemble, is the Instrumentation & Control System (I&C). It consists of all the sensors, actuators, controllers, and man machine interfaces necessary for the systems to perform their duties according to the user needs. I&C is specified in term of the functionalities (functions) that it provides. For good practical and regulatory reasons, functions are divided into the following categories: control, machine-protection and safety. For each category different design and quality requirements are applied both to comply with regulatory prescription and to better focus the engineering costs.

Safety I&C provides functions meant to help reducing any harm risk to people. Machine protection functions aim at reducing the total cost of ownership both by reducing the chance or the consequence of a plant failure and by reducing downtime. Control I&C functions are those necessary to help implement the needed features of the facility.

Architecture

Architectural blocks

DICS architecture design identifies the components of DICS and provides a brief description of the interfaces among components.

The first architectural choice is the division of DICS between central systems and plant systems. Plant System I&C contains sensors and actuators and performs all the functions necessary for the standalone operation of one part of the plant (for example a PF power supply or the electrical distribution). Central I&C Systems are those instead concerned with the coordinated operation of Plant Systems.

The second architectural choice is the division of central DICS into four major systems on the basis of the main categorisation of functions:

- COSS Central Occupational Safety System
- CMPS Central Machine Protection System (hard investment protection functions)

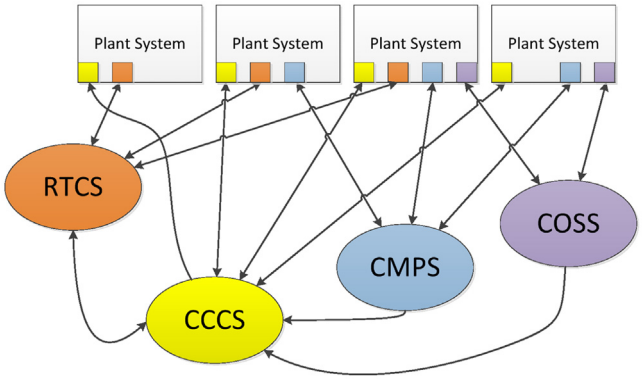

Fig. 5. DICS architecture.

- RTCS Real Time Control System (network of collaborating Systems)
- CCCS Central Command and Control Systems (including data collection and monitoring)

CCCS and RTCS both provide control I&C functions, but are distinct because the former provides functions necessary for the configuration, coordination and activation of systems, while the latter provides functions necessary for the operation of systems.

For large Plant Systems the same subdivision used for the central systems, should also be applied when it leads to a more rational development, easier to manage and maintain.

Main interfaces

Interfaces may exist between a Plant System and any of the central systems. Interfaces among Plant Systems are provided by the RTCS network. Direct interfaces are possible but should be limited.

For cost and maintenance reasons, one important objective is to design and manufacture Plant Systems using as much as possible industrial standards. For this reason the interfaces between Plant Systems and CCCS will employ as much as possible open industrial standards like open platform communications (OPC) over a dedicated network infrastructure CCCSN. To collect large volumes of experimental data DTT will instead employ a custom distributed Transmission Control Protocol (TCP) based client server system like for instance MDSplus [69].

Safety and Machine Protection functions will be implemented as close as possible to the Plant and will be organised around the affected actuator. When measurements from a different plant are needed, the needed sensors will be either shared or transferred functionally to the needing system. Interfaces to the CMPS and COSS will be kept to the minimum and implemented employing the simplest mechanism.

RTCS is a set of collaborating Plant Systems and Systems intercommunicating over a dedicated real-time network (RTN). This network will have multi-star topology and employ multicast User Datagram Protocol (UDP) with a custom application layer. In order to allow qualification of the network, the traffic will be stationary, with the same pattern of packets repeating with a frequency faster than 10 Hz. This means that all the transmitters will be synchronised with common central clock and will send data with frequencies multiple of 10 Hz. Packet content and multicast circuits will be prescribed centrally.

Control hierarchy

Fig. 5 shows a flat 2 level architecture for DICS where all the plant systems occupy one level and all the central systems the other. In fact Plant Systems will be internally organised hierarchically, possibly with a distinct number of levels for control, investment protection and safety. The specific architecture will be driven by the operational needs, with as many subdivisions as needed independent operations of subsystems during commissioning or maintenance. Safety and machine protection will typically require a more monolithic implementation as segregated protection is only possible if true segregation of the sub-plants is implemented.

Within the central systems also limited hierarchy will be implemented. The main design driver will be the need to allow both coordinated and segregated operation of groups of plant systems (for instance during commissioning).

Preliminary technological choice

For Plant System, a standard industrial solution will be preferred: PLCs and remote IOs interconnected via a field bus (for instance PROFINET). No specific brand of PLC will be selected, but the focus will be on openness and on interoperability.

For all the functions where PLCs are not applicable, the choice will be a solution employing PC Server Machines and remote IO (PCI-express or Ethernet) on adequate chassis (for instance ATCA or compact PCI-express).

Whenever demand for reaction time or computational speed exceeds what the above hardware can provide, solutions based on FPGA or parallel processors (GPUs) will be investigated.

For investment protection and safety, in addition to the above consideration, for the hardware and software tools, qualification to relevant standards will be required.

5. Final remarks

An overview of the diagnostic and control system conceived so far for DTT has been given. Focussing on the specific mission of the machine, diagnostic and control system will provide the tools to experiment and optimize various solutions for the power exhaust control, involving tailored magnetic topologies, highly radiative regimes, advanced materials and with a particular vocation to develop model driven schemes for power exhaust control in preparation of DEMO.

Acknowledgements

This work has been carried out within the framework of the EURO fusion Consortium and has received funding from the Euratom research and training programme 2014–2018 under grant agreement No. 633053. The views and opinions expressed herein do not necessarily reflect those of the European Commission.

References

[1] A. Pizzuto, et al., Divertor Tokamak Test Facility Project Proposal, ENEA Editor, 2015, ISBN: 978-88-8286-318-0.
[2] F. Felici, et al., Fusion Eng. Des. 89 (2014) 165–176.
[3] E.J. Strait, et al., Fusion Sci. Technol. 53 (2008) 304–334.
[4] G. Vayakis, et al., Rev. Sci. Instrum. 83 (2012) 10D712.
[5] JET Magnetic Diagnostics, http://users.euro-fusion.org/pages/mags/index.html.
[6] D. Testa, et al., IEEE Trans. Plasma Sci. 38 (2010) 284–294.
[7] G. Vayakis, et al., J. Nucl. Mater. 417 (2011) 780–786.
[8] Plasma Phys. Contr. Fusion 59 (2017) 014044.
[9] P. Innocente, et al., Rev. Sci. Instrum. 63 (1992) 4996.
[10] S. Peruzzo, et al., R&D on ITER in-vessel magnetic sensors, Fusion Eng. Des. 88 (2013) 1302–1305.
[11] O.N. Jarvis Plasma, Phys. Control. Fusion 36 (1994) 209.
[12] X. Zhang, et al., Nucl. Fusion 54 (2014) 104008.
[13] C. Hellesen, et al., Plasma Phys. Contr. Fusion 52 (2010) 085013.
[14] J. Eriksson, et al., Nucl. Fusion 55 (2015) 123026.
[15] C. Cazzaniga, et al., Rev. Sci. Instrum. 85 (2014) 043506.
[16] (a) M. Nocente, et al., Rev. Sci. Instrum. 60 (2014) 11E108;
(b) M. Nocente, et al., IEEE Trans. Nucl. Sci. 60 (2013) 1408.
[17] M. Tardocchi, et al., Phys. Rev. Lett. 107 (2011) 205002.
[18] M. Tardocchi, M. Nocente, G. Gorini, Plasma Phys. Control. Fusion 55 (2013) 074014.
[19] L. Giannone et al, Plasma Phys. Contr. Fusion 47 (2005) 2123.
[20] M. Bernert, et al., Rev. Sci. Instrum. 85 (2014) 033503.
[21] M.L. Reinke, I.H. Hutchinson, Rev. Sci. Instrum. 79 (2008) 10F306.
[22] J. Howard, JINST 10 (2015) P09023.

[23] G. Maddaluno, et al., Espoo Finland, 40th EPS Conference on Plasma Phys., vol. 37D, 2013, p. P5.102 http://ocs.ciemat.es/EPSAP/pdf/P5.102.pdf.
[24] H.K. Gulati, H. Dave, F. Di Maio, A. Wallander, Fusion Eng. Des. 85 (2010) 549.
[25] G. Gennacchi, A. Taroni, JETTO: A Free Boundary Plasma Transport Code (Basic Version), vol. 5, Tech. rep. ENEA, RT/TIB, Rome (Italy), 1988.
[26] G. Pereverzev, P. Yushmanov, ASTRA Automated System for Transport Analysis in a Tokamak, Tech. Rep. Max-Planck-Institut fur Plasmaphysik, Garching (Germany), 2002.
[27] D. Humphreys, et al., Fusion Eng. Des. 83 (2–3) (2008) 193–197.
[28] G. De Tommasi, et al., IEEE Trans. Plasma Sci. 35 (3) (2007) 709–723.
[29] T. Bellizio, et al., Fusion Eng. Des. 86 (2011) 1026–1029.
[30] S. Peruzzo, et al., Fusion Eng. Des. 84 (2009) 1495–1498.
[31] F.M. Callier, C.A. Desoer, Linear System Theory, Springer, Verlag, 1991.
[32] R. Albanese, F. Villone, Nucl. Fus. 38 (5) (1998) 723–738.
[33] R. Albanese, R. Ambrosino, M. Mattei, Fusion Eng. Des. 96–97 (2015) 664–667.
[34] G. Marchiori, et al., Fusion Eng. Des. 108 (2016) 81–91.
[35] R. Albanese, et al., Fusion Eng. Des. 74 (1–4) (2005) 627–632.
[36] G. Calabrò, et al., Nucl. Fusion 55 (8) (2015) 083005.
[37] A. Neto, et al., Fusion Eng. Des. 96–97 (2015) 887–890.
[38] R. Wenninger, et al., Nucl. Fusion 55 (6) (2015) 063003–063307.
[39] M. Romanelli, et al., Plasma Fusion Res. 9 (special issue 2) (2014), 3403023-1-4.
[40] G. Ambrosino, M. Ariola, G. De Tommasi, A. Pironti, IEEE Trans. Contr. Sys. Tech. 19 (2) (2011) 376–381.
[41] M. Ariola, A. Pironti, IEEE Control Syst. Mag. 25 (5) (2005) 65–75.
[42] G. De Tommasi, et al., J. Fusion Energy 33 (2) (2014) 233–242.
[43] R. Albanese, et al., A MIMO architecture for integrated control of plasma shape and flux expansion for the EAST tokamak, in: Proc. of the 2016 IEEE Multi-Conf. Syst. Contr., Buenos Aires, Argentina, 2016.
[44] G. De Tommasi, S. Galeani, A. Pironti, G. Varano, L. Zaccarian, Automatica 47 (5) (2011) 981–987.
[45] A. Lampasi, et al. The DTT device: power supplies and electrical distribution system, Fusion Eng. Des. This special issue.
[46] A. Huber, et al., J. Nucl. Mater. 363–365 (2007) 365, Proc. 17th Int. Conf. on Plasma Surface Interactions in Controlled Fusion Devices (PSI-17), Hefei, China, May 2006.
[47] C. Grisolia, et al., J. Nucl. Mater. 275 (1) (1999) 95–100.
[48] J.P. Gunn, et al., Plasma Phys. Contr. Fusion 42 (2000) 557.
[49] L. Costanzo, et al., Detachment Control by Heat Flux Analysis on Tore Supra, vol. 25 A, ECA, 2001, pp. 197–200.
[50] J. Neuhauser, et al., Plasma Phys. Contr. Fusion 37 (1995) A37–A51.
[51] H.Y. Guo, et al., J. Nucl. Mater. 415 (2011) S369–S374.
[52] A.V. Chankin, et al., Plasma Phys. Contr. Fusion 44 (2002) A399–A405.
[53] The JET team (presented by R.D. monk), "Recent results from divertor and SOL studies at JET", IAEA-CN-69/EX6/4, in: Proc. 17th IAEA Fusion Energy Conference, Yokohama, Japan, 19–24 October, 1998.
[54] J.L. Terry, et al., Phys. Plasma 5 (1998) 1759–1766.
[55] V.A. Soukhanovskii, et al., J. Nucl. Mater. 363–365 (2007) 432–436.
[56] V.A. Soukhanovskii, et al., Phys. Plasmas 16 (2009) 022501.
[57] G. Hommen, et al., Nuclear Fusion 54 (7) (2014) 073018.
[58] Hommen, Rev. Sci. Instrum. 11 (81) (2010) 113504.
[59] J.F. Drake, Phys. Fluids 30 (1987) 2429–2433.
[60] E. Kolemen, J. Nucl. Mater. 463 (2015) 1186 (48693).
[61] C. Angioni, et al., Nucl. Fusion (2017) 022009.
[62] L. Figini, et al., 43rd Conf. Plasma Phys Contr. Fusion, Leuven, Belgium, 2017 http://ocs.ciemat.es/EPS2016PAP/pdf/P4.072.pdf.
[63] S. Mastrostefano, P. Bettini, T. Bolzonella, M. Furno Palumbo, Y.Q. Liu, Matsunaga, R. Specogna, M. Takechi, F. Villone, Fusion Eng. Des. 96–97 (2015) 659.
[64] D.G. Whyte, et al., Nucl. Fusion 50 (2010) 105005.
[65] K.H. Burrell, M.E. Austin, D.P. Brennan, et al., Plasma Phys. Control. Fusion 44 (2002) A253.
[66] W.M. Solomon, P.B. Sneyder, A. Bortolon, et al., Phys. Plasmas 23 (2016) 056105.
[67] T.H. Osborne, G.L. Jackson, Z. Yan, et al., Nucl. Fusion 55 (2015) 063018.
[68] J. Li, H.Y. Guo, B.N. Wan, et al., Nat. Phys. 9 (2013) 817–821.
[69] G. Manduchi, T. Fredian, J. Stillerman, Fusion Eng. Des. 89 (2014) 775–779.